THE EUROPEAN
PHYSICAL JOURNAL C

CrossMark

Quasinormal modes and thermodynamics of linearly charged BTZ black holes in massive gravity in (anti) de Sitter space-time

P. Prasia[a] (iD), **V. C. Kuriakose**[b]

Department of Physics, Cochin University of Science and Technology, Kochi 682022, India

Abstract In this work we study the Quasi-Normal Modes (QNMs) under massless scalar perturbations and the thermodynamics of linearly charged BTZ black holes in massive gravity in the (Anti)de Sitter ((A)dS) space-time. It is found that the behavior of QNMs changes with the massive parameter of the graviton and also with the charge of the black hole. The thermodynamics of such black holes in the (A)dS space-time is also analyzed in detail. The behavior of specific heat with temperature for such black holes gives an indication of a phase transition that depends on the massive parameter of the graviton and also on the charge of the black hole.

1 Introduction

Einstein's General Theory of Relativity (GTR) helped us to understand the dynamics of the universe. But there are some fundamental issues that could not be addressed in GTR [1] and several attempts are being made to modify the GTR to find solutions to these fundamental issues. GTR is a theory based on massless gravitons with two degrees of freedom. A way of modifying GTR essentially implies giving mass to the graviton and in the present study we consider massive gravity. The attempts to modify GTR resulted in the so called 'Alternative Theories of Gravity' [2]. Theories concerning the breaking up of Lorentz invariance and spin had been explored in depth [3]. The first attempt toward constructing a theory of massive gravity was done by Fierz and Pauli [4] in 1939. Only by the 1970s researchers showed interests in this formulation. van Dam and Veltman [5] and Zhakharov [6] in 1970 showed that a theory of massive gravity could never resemble GTR in the massless limit and this is known as vDVZ discontinuity. Later Vainshtein [7] proposed that the linear massive gravity can be recovered to GTR through the 'Vainshtein Mechanism' at small scales

by including non-linear terms in the massive gravity action. But this model suffers from a pathology called a 'Boulware–Deser' (BD) ghost and was ruled out on the basis of solar system tests [8]. Later a class of massive gravity was proposed by de Rham, Gahadadze and Tolley, called 'dRGT massive gravity', that evades the 'BD ghost' [9,10]. In this theory the mass terms were produced by a reference metric. A class of black hole solutions in the dRGT model and their thermodynamic behavior were studied later [11–13]. Vegh [14] proposed another type of massive gravity theory. This theory was similar to dRGT except that the reference metric was a singular one. Using this theory he showed that graviton behaves like a lattice and showed the existence of Drude peak. This theory was found to be ghost-free and stable for arbitrary singular metric.

It was Hawking [15] who first showed that a black hole thermally radiates and who calculated its temperature. Thereafter the thermodynamics of black holes got wide acceptance and interests among researchers. The question of thermal stability is one of the important aspects of black hole thermodynamics [16,17]. The thermodynamics and phase transition shown by black holes have been largely explored for almost all space-times [18–21] and references cited therein. In the realm of massive gravity also, the thermodynamics and phase transitions have been studied for different black hole space-time [22,23].

Recently there has been a growing interest in the asymptotically Anti de Sitter (AdS) space-times. The black hole solution proposed by Banados–Teitelboim–Zanelli (BTZ) in (2 + 1) dimensions deals with asymptotically AdS space-time and has got well defined charges at infinity, mass, angular momentum and makes a good testing ground especially when one would like to go beyond the asymptotic flatness [24]. Another interesting aspect of the black hole solution is related to the AdS/CFT (Conformal Field Theory) correspondence. In (2+1) dimensions, the BTZ black hole solution is a space-time of constant negative curvature and it differs from

[a] e-mail: prasiapankunni@cusat.ac.in

[b] e-mail: vck@cusat.ac.in

the AdS space time in its global properties [25]. The thermodynamic phase transitions and area spectrum of the BTZ black holes are studied in detail [26–28]. Also, the charged BTZ black hole solutions are studied for the phase transition in Refs. [29,30].

Another important aspect of a black hole is its Quasi-Normal Modes (QNMs). QNMs can be found as a solution to the perturbed field equation corresponding to the scalar, gravitational and electromagnetic perturbations of black hole space-time. It comes out as a natural response to these perturbations. The existence of QNMs was first found by Visweshwara [31] and attempts were made to find QNMs for different space-times. QNMs of black holes were first numerically computed by Chandrasekhar and Detweiler [32]. It was Cardoso and Lemos [33] who first calculated the exact QNMs of the BTZ black holes. They have found out both analytical and numerical solutions to the BTZ black hole perturbation for non-rotating BTZ black holes. It is interesting to note that they got exact analytical solutions to the wave equation that made BTZ an important space-time where one can prove or disprove the conjectures relating to QNMs, critical phenomena or area quantization.

Electromagnetic field can be a good choice of source for getting deep insights into the three dimensional massive gravity. In this paper the QNMs, the associated phase transition and thermodynamics of BTZ black hole in massive gravity in the presence of Maxwell's field has been studied. The paper is organized as follows: in Sect. 2, the QNMs of a linearly charged BTZ black holes in massive gravity are studied for different values of the massive parameter of graviton and charge for de Sitter and Anti de Sitter space-times. The behavior of quasi-normal frequencies and phase transition are also dealt with. Section 3 deals with the thermodynamics of such black holes. The influence of the massive parameter and charge of the black hole on the various thermodynamic factors are studied. Section 4 concludes the paper.

2 Quasi-normal modes of a linearly charged BTZ black hole in massive gravity

In this section, we first look into the perturbation of black hole space-time by a scalar field. For a linearly charged black hole, the Einstein–Maxwell action in $(2 + 1)$ dimension is given by [34],

$$S_{\text{EM}} = \frac{1}{16\pi G} \int \mathrm{d}^3x \sqrt{-g} \left[R + \frac{2}{l^2} - 4\pi G F_{\mu\nu} F^{\mu\nu} \right], \tag{1}$$

where R is the Ricci scalar, $F_{\mu\nu} = \partial_\mu A_\nu - \partial_\nu A_\mu$ is the Faraday tensor, A_μ is the gauge potential, and $F^{\mu\nu} F_{\mu\nu}$ is the Maxwell invariant. The action given above can be generalized

to include the massive gravity for the de Sitter space-time as [35],

$$S = \frac{-1}{16\pi} \int \mathrm{d}^3x \sqrt{-g} [R + 2\Lambda + L(\mathcal{F})$$
$$+ m^2 \sum_i^4 c_i \mathcal{U}_i(g, f)], \tag{2}$$

where $\mathcal{F} = F^{\mu\nu} F_{\mu\nu}$, L is an arbitrary Lagrangian of electrodynamics, $\frac{1}{l^2} = \Lambda$, the cosmological constant in the de Sitter (dS) space-time, m is the massive parameter of the graviton, c_is are constants, $f_{\mu\nu}$ is the second metric and is chosen to be a fixed symmetric tensor here. There is no dynamics for the metric f. $\mathcal{U}_i$s are symmetric polynomials of the eigenvalue of the 3×3 matrix $\mathcal{K}^\mu_\nu = \sqrt{g^{\mu\alpha} f_{\alpha\nu}}$, given by [14,23]

$\mathcal{U}_1 = [\mathcal{K}]$

$\mathcal{U}_2 = [\mathcal{K}]^2 - [\mathcal{K}^2]$,

$\mathcal{U}_3 = [\mathcal{K}]^3 - 3[\mathcal{K}][\mathcal{K}^2] + 2[\mathcal{K}^3]$,

$\mathcal{U}_4 = [\mathcal{K}]^4 - 6[\mathcal{K}]^2[\mathcal{K}^2] + 8[\mathcal{K}^3][\mathcal{K}] + 3[\mathcal{K}^2]^2 - 6[\mathcal{K}^4]$,

where $[\mathcal{K}] = Tr(\mathcal{K}) = \mathcal{K}^\mu_\mu$. Varying (2) with respect to the metric $g_{\mu\nu}$, we can obtain the gravitation field equation:

$$G_{\mu\nu} + \Lambda g_{\mu\nu} - \frac{1}{2} g_{\mu\nu} L(\mathcal{F}) - 2 L_{\mathcal{F}} F_{\mu\rho} F^\rho_\nu + m^2 \mathcal{X}_{\mu\nu} = 0, \tag{3}$$

where

$$G_{\mu\nu} = R_{\mu\nu} - \frac{1}{2} g_{\mu\nu} R, \quad L_{\mathcal{F}} = \frac{\mathrm{d}L(\mathcal{F})}{\mathrm{d}\mathcal{F}}$$

and

$$\mathcal{X}_{\mu\nu} = \frac{-c_1}{2} (\mathcal{U}_1 g_{\mu\nu} - \mathcal{K}_{\mu\nu}) - \frac{c_2}{2} (\mathcal{U}_2 g_{\mu\nu} - 2\mathcal{U}_1 \mathcal{K}_{\mu\nu} + 2\mathcal{K}^2_{\mu\nu})$$
$$- \frac{-c_3}{2} (\mathcal{U}_4 g_{\mu\nu} - 4\mathcal{U}_3 \mathcal{K}_{\mu\nu} + 12\mathcal{U}_2 \mathcal{K}^2_{\mu\nu}$$
$$- 24\mathcal{U}_1 \mathcal{K}^3_{\mu\nu} + 24\mathcal{K}^4_{\mu\nu}). \tag{4}$$

where the $f_{\mu\nu}$ terms that comes out of varying the action is absorbed to give the potentials $\mathcal{U}_i$ during simplification. To obtain static charged black hole solution we consider the 3 dimensional metric,

$$\mathrm{d}s^2 = -f(r)\mathrm{d}t^2 + f^{-1}(r)\mathrm{d}r^2 + r^2\mathrm{d}\theta^2. \tag{5}$$

To get an exact solution for this metric, the following reference metric is employed [14]:

$$f_{\mu\nu} = \mathrm{diag}(0, 0, c^2), \tag{6}$$

where c is a positive constant.

For a $(2 + n)$ dimensional massive gravity, $\mathcal{U}_i$s can be written as [23]

$\mathcal{U}_1 = n\,c/r$,

$\mathcal{U}_2 = n(n - 1)c^2/r^2$,

$\mathcal{U}_3 = n(n - 1)(n - 2)c^3/r^3$,

$\mathcal{U}_4 = n(n - 1)(n - 2)(n - 3)c^4/r^4$.

Now, for $(2 + 1)$ dimensional massive gravity, we therefore obtain

$$\mathcal{U}_1 = \frac{c}{r},$$
$$\mathcal{U}_2 = \mathcal{U}_3 = \mathcal{U}_4 = 0.$$

The Lagrangian of the Maxwell field is chosen as $L(\mathcal{F}) = -\mathcal{F}$ and the radial electric field is chosen as

$$h(r) = \sqrt{Q} \ln\left(\frac{r}{\alpha}\right),$$

where Q is an integration constant which is related to the charge of the black hole and α ia an arbitrary constant that has got the dimension of length. Using (3) and (5) for getting exact solutions for the metric function leads to the set of differential equations, corresponding to the tt(or rr) and $\theta\theta$ components, respectively, given by

$$rf'(r) + 2r^2\Lambda + 2Q - m^2cc_1r = 0,$$
$$\frac{r^2}{2}f''(r) + \Lambda r^2 - Q = 0.$$

Solving these equations will lead to the metric function, in the dS space as [34,35]

$$f(r) = \Lambda r^2 - m_0 - 2Q \ln\frac{r}{\alpha} + m^2cc_1r, \tag{7}$$

where m_0 is related to the mass of the black hole, Q is the charge parameter, α is an arbitrary constant, and c_1 is a constant. For an Anti de Sitter space, Λ will take negative values. From the metric function, it can be understood that the contribution of the massive term depends on the sign of c_1. In this Section, we look into the behavior of QNMs of the linearly charged BTZ black hole with metric function given by (7). A massless scalar field perturbation in this space-time satisfies the Klein–Gordon equation,

$$\frac{1}{\sqrt{-g}}\frac{\partial}{\partial x^a}\left(g^{ab}\sqrt{-g}\frac{\partial}{\partial x^b}\right)\Phi = 0, \tag{8}$$

which on expanding gives

$$\frac{1}{f(r)}\frac{\partial^2\Phi}{\partial t^2} - \frac{\partial}{\partial r}f(r)\frac{\partial\Phi}{\partial r} - \frac{1}{r^2}\frac{\partial^2\Phi}{\partial\phi^2} = 0. \tag{9}$$

The metric function $f(r)$ is given by (7). To separate the angular variables, we make use of the ansatz

$$\Phi = \frac{R(r)}{r}e^{-i\omega t}e^{im_l\phi}, \tag{10}$$

where ω is the frequency, m_l is the angular momentum quantum number. Using the above ansatz, the Klein–Gordon equation can be re-written as

$$\frac{d^2R}{dr^2} + \frac{f'(r)}{f(r)}\frac{dR}{dr} + \left[\frac{\omega^2}{f(r)^2} - \frac{(\frac{m_l^2}{r^2} - \frac{2Q}{r^2} + \frac{cc_1m}{r})}{f(r)}\right]R = 0. \tag{11}$$

Quasi-normal modes are in going waves at the event horizon and outgoing waves at the cosmological horizon, leading to the boundary condition

$$R \to \begin{cases} e^{i\omega r}, & \text{as } r \to \infty, \\ e^{-i\omega r}, & \text{as } r \to -\infty. \end{cases} \tag{12}$$

Making a variable change $r \to 1/\xi$, the wave equation becomes

$$\frac{d^2R}{d\xi^2} + \frac{p'}{p}\frac{dR}{d\xi} + \left[\frac{\omega^2}{p^2} - \frac{2Q + \frac{2\Lambda}{\xi^2} - \frac{cc_1m}{\xi} - m_l^2}{p}\right]R = 0, \tag{13}$$

where

$$p = M\xi^2 - cc_1m\xi + 2Q\xi^2\ln\left(\frac{1}{\alpha\xi}\right) + \Lambda, \tag{14}$$

$$p' = 2(M - Q)\xi - cc_1m + 4Q\xi\ln\left(\frac{1}{\alpha\xi}\right). \tag{15}$$

This black hole has an extreme outer horizon and a naked singularity [35]. In order to solve the wave equation, the singularity has to be scaled out. Here, we first scale out the divergent behavior at the outer horizon taking [36]

$$R(\xi) = e^{i\omega\xi}u(\xi), \tag{16}$$

where

$$e^{i\omega\xi} = (\xi - \xi_1)^{\frac{i\omega}{2\kappa_1}} \tag{17}$$

and

$$\kappa_1 = \frac{1}{2}\frac{\partial f}{\partial r} \mid r \to r_1 \tag{18}$$

is the surface gravity at the outer horizon. The master equation then will take the form

$$pu'' + (p' - 2i\omega)u' - \left(2Q - \frac{2\Lambda}{\xi^2} - \frac{cc_1m}{\xi} - m_l^2\right)u = 0. \tag{19}$$

This can be viewed as

$$u'' = \lambda_0(\xi)u' + s_0(\xi)u, \tag{20}$$

with

$$\lambda_0 = -\frac{(p' - 2i\omega)}{p}, \tag{21}$$

$$s_0 = \frac{\left(2Q - \frac{2\Lambda}{\xi^2} - \frac{cc_1m}{\xi} - m_l^2\right)}{p}. \tag{22}$$

We employ the Improved Asymptotic Iteration Method (Improved AIM) explained in Refs. [37–39].

The Asymptotic Iteration Method (AIM) was proposed initially for finding solutions of the second order differential equations of the form

$$Y''(x) - \lambda_0(x)Y'(x) - s_0(x)Y(x) = 0,$$

where $\lambda_0(x)$ and $s_0(x)$ are coefficients of the differential equation and are well defined functions and sufficiently differentiable. By differentiating the above expression n times, we arrive at the expression

$$Y^{(n)}(x) - \lambda_{n-2}(x)Y'(x) - s_{n-2}(x)Y(x) = 0,$$

where the new coefficients in terms of the old ones are given as

$$\lambda_n(x) = \lambda'_{n-1} + \lambda_{n-1}\lambda_0 + s_{n-1},$$
$$s_n(x) = s'_{n-1} + s_0\lambda_{n-1},$$

with $n = 1, 2, 3, \ldots$. By introducing the asymptotic concept that for sufficiently large values of n,

$$\frac{s_n}{\lambda_n} = \frac{s_{n-1}}{\lambda_{n-1}} \equiv \alpha,$$

where α is a constant, we can arrive at the quantization condition,

$$\lambda_n(x)s_{n-1}(x) - \lambda_{n-1}(x)s_n(x) = 0.$$

It can be seen from (21) that λ_0 contains the quasi normal frequencies. So, the quantization condition given by (23) can be used to determine the quasi-normal frequencies of the black hole.

In this work we have employed the Improved AIM wherein the Taylor expansion of the coefficients are used. For that, λ_n and s_n are expanded in a Taylor series around the point at which AIM is performed, x',

$$\lambda_n(x') = \sum_{i=0}^{\infty} c_n^i (x - x')^i,$$
$$s_n(x') = \sum_{i=0}^{\infty} d_n^i (x - x')^i,$$

where c_n^i and d_n^i are the ith Taylor coefficients of $\lambda_n(x')$ and $s_n(x')$, respectively. Substitution of Eqs. (9) and (10) in (5) and (6) leads to the recursion relation for the coefficients as

$$c_n^i = (i+1)c_{n-1}^{i+1} + d_{n-1}^i + \sum_{k=0}^{i} c_0^k c_{n-1}^{i-k},$$
$$d_n^i = (i+1)d_{n-1}^{i+1} + \sum_{k=0}^{i} d_0^k c_{n-1}^{i-k}.$$

Applying the Taylor expanded coefficients, the quantization condition can be rewritten as

$$d_n^0 c_{n-1}^0 - d_{n-1}^0 c_n^0 = 0. \tag{23}$$

This gives a set of recursion relations that do not require any derivatives. The coefficients given by c_n^i and d_n^i can be computed by starting at $n = 0$ and iterating up to $(n+1)$ until the desired number of recursions are reached. The quantization condition contains only the $i = 0$ term. So, only the coefficients with $i < N - n$ where N is the maximum number of iterations to be performed needs to be determined.

It can be seen from (19) that the coefficient of u' includes the frequency ω. Therefore the quantization condition given by (23) can be used to find the ω of (19) by iterating to some n maximum. In this paper we have calculated QNMs using the Mathematica Notebook [40].

In Table 1 we list the quasi-normal frequencies of the black hole in the de Sitter space-time for $m = 1$, $m = 1.05$, and $m = 1.1$ for different values of the cosmological constant, calculated using the improved AIM discussed above. We have used the parameter values $Q = 0.25$, $m_l = 1$, $\alpha = 1$, $c = 1$, and $c_1 = 1$. In the numerical calculations we have used 15 iterations. It is observed that the behavior of the quasi-normal frequencies, i.e., the way in which quasi-normal frequencies vary with Λ, change after a particular Λ

Table 1 QNMs of linearly charged BTZ black hole for different values of the massive parameter for dS space-time with $Q = 0.25$

| $m = 1$		$m = 1.05$		$m = 1.1$	
Λ	$\omega = \omega_R + \omega_I$	Λ	$\omega = \omega_R + \omega_I$	Λ	$\omega = \omega_R + \omega_I$
0.05	$1.10826 - 0.11372i$	0.13	$2.34196 - 0.20795i$	0.19	$4.17236 - 1.06710i$
0.06	$1.11679 - 0.12335i$	0.15	$2.44520 - 0.20739i$	0.21	$4.27438 - 1.24924i$
0.07	$1.12571 - 0.13415i$	0.17	$2.54513 - 0.20066i$	0.23	$4.36708 - 1.46493i$
0.08	$1.13484 - 0.14622i$	0.19	$2.63890 - 0.19441i$	0.25	$4.44633 - 1.71966i$
0.09	$1.14390 - 0.15966i$	0.20	$2.68389 - 0.19356i$	0.27	$4.50586 - 2.02037i$
0.10	$1.15262 - 0.17447i$	0.21	$2.72810 - 0.19347i$	0.28	$4.52540 - 2.19059i$
0.11	$1.57071 - 0.17563i$	0.22	$2.77213 - 0.19538i$	0.29	$0.54837 - 2.25384i$
0.12	$1.57561 - 0.17204i$	0.23	$2.81604 - 0.19882i$	0.30	$0.50212 - 2.32018i$
0.13	$1.58260 - 0.16856i$	0.25	$2.90460 - 0.20967i$	0.31	$0.45065 - 2.39119i$
0.14	$1.59172 - 0.16559i$	0.27	$2.99477 - 0.22423i$	0.32	$0.39409 - 2.46833i$
0.15	$1.60312 - 0.16277i$	0.29	$3.08568 - 0.24039i$	0.33	$0.33391 - 2.55151i$
0.16	$1.61655 - 0.16277i$	0.31	$3.25912 - 0.27670i$	0.34	$0.26958 - 2.63657i$
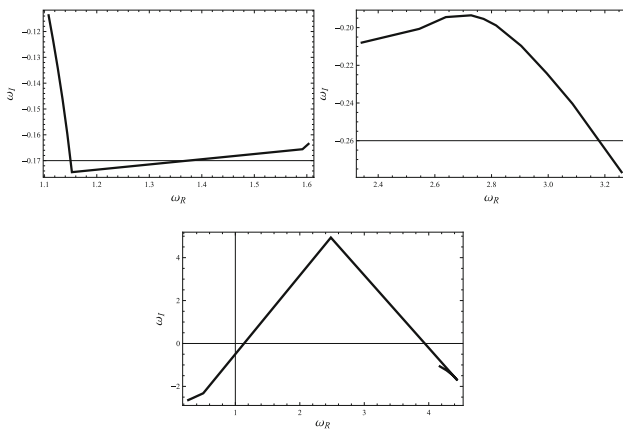
Fig. 1 QNM behavior for linearly charged BTZ black hole for $Q = 0.25$ the massive parameter value $m = 1, 1.05, 1.1$. The sudden change in the slope can be treated as indicative of a possible phase transition.
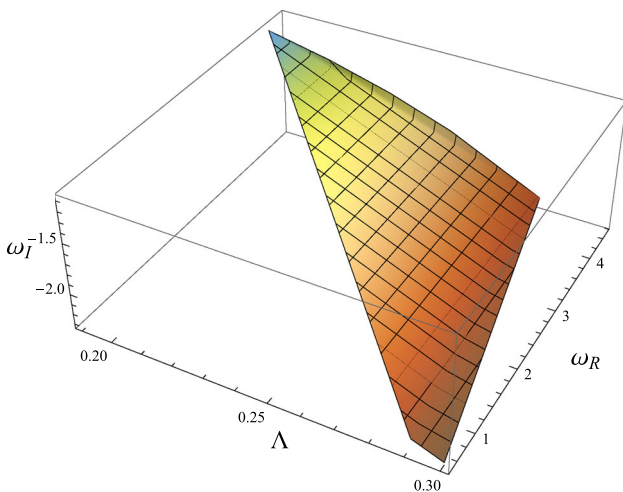

Fig. 2 The behavior of QNMs with Λ calculated in Table 1 for $m = 1.1$ for the dS space-time

value. This change in behavior is shown in the table by a horizontal line as a separator. This sudden change in behavior happens at $\Lambda = 0.1$ for $m = 1$, at $\Lambda = 0.21$ for $m = 1.05$, and at $\Lambda = 0.28$ for $m = 1.1$. The behavior of the QNMs, ω_R versus ω_I, for $m = 1, 1.05$ and 1.1 given by Table 1 are plotted in Fig. 1.

From the figures it can be clearly seen that the slope of the curve changes suddenly at some transition point for $m = 1, 1.05, 1.1$. This behavior can be treated as a clear indication of a phase transition. However, for the same values of the constant parameters this phase transition occurs at different values of Λ for the different m values. The higher the value of m, the higher the value of Λ at which the phase transition occurs. As an example, the variation of the QNMs (ω_R and ω_I) with Λ for the massive parameter $m = 1.1$ is shown in Fig. 2.

In Table 2, we show the quasi-normal frequencies are calculated for $Q = 0.35$ for $m = 0.9$, $m = 0.95$ and $m = 1.0$ with the parameter values $m_l = c = c_1 = 1$. The behavior of these QNMs (ω_R versus ω_I) are shown in Fig. 3. Just like in the case where $Q = 0.25$, here also there is a sudden change in the slope of the curve after a particular Λ indicating a phase transition.

Thus for both values of Q the black hole shows a phase transition for the dS space-time. We can see from Tables 1 and 2 that for the value $m = 1.0$ the phase transition happens at different values of Λ for the $Q = 0.25$ and $Q = 0.35$ cases.

In Table 3 we show the QNMs calculated for an AdS space time for the massive parameter values $m = 1, 1.05, 1.1$ with $Q = 0.1$, $\alpha = 1$, $c = 1$, $c_1 = 1$. From Table 3, it can be observed that the ω_R and ω_I continuously decrease and after reaching a particular Λ, the real and imaginary parts suddenly increases and then continuously decreases. This jump can be treated as an indication of an inflection point.

The ω_R versus ω_I for these cases are plotted in Fig. 4. In this case there is no drastic change in the slope and the behavior of the QNMs are similar for all values of m. Hence it can be inferred that there will be no phase transition.

In Table 4 we have calculated the QNMs for the AdS space time for the massive parameter values $m = 0.95, 1, 1.05$ with $Q = 0.25$, $\alpha = 1$, $c = 1$, $c_1 = 1$. Figure 5 shows the behavior of quasi-normal frequencies, ω_R versus ω_I, for the above case. It can be seen that there is a sudden change in the slope of the curve after reaching a particular Λ indicating a possible phase transition.

For $Q = 0.1$ the AdS black hole space-time does not show any phase transition behavior but for $Q = 0.25$ it is found to be showing a phase transition behavior. Thus it can be inferred that the phase transition behavior depends on the charge Q.

Now, it would be interesting to check the variation of QNMs with Q. Table 5 shows the quasi-normal frequencies calculated for different charges Q in dS space-time for a fixed Λ. It can be seen that the behavior of quasi-normal frequency changes frequently. The phase transition behavior is highly dependent on the charge. The phase does not remain the same for a wide range of charge and hence the phase transition is found to happen frequently over a range of charges. This variation is plotted in Fig. 6.

The variation of QNMs with charge calculated for a fixed Λ in the AdS case is shown in Table 6.

It can be seen that, compared to the dS case, phase transition does not happen frequently, i.e., the phases remain the same for most of the values of charge and a transition happens only for certain small range of charge values. This behavior is plotted in Fig. 7.

Thus, in this section, the QNMs for a linearly charged black hole in massive gravity are calculated for the dS and

Table 2 QNMs of linearly charged BTZ black hole for different values of the massive parameter for dS space-time with $Q = 0.35$

| $m = 0.9$		$m = 0.95$		$m = 1.0$	
Λ	$\omega = \omega_R + \omega_I$	Λ	$\omega = \omega_R + \omega_I$	Λ	$\omega = \omega_R + \omega_I$
0.09	$0.898571 - 0.0783066i$	0.05	$1.16072 - 0.0686295i$	0.01	$1.68971 - 0.172263i$
0.10	$0.901026 - 0.0798863i$	0.06	$1.18398 - 0.0690504i$	0.015	$1.69779 - 0.581786i$
0.11	$0.902855 - 0.0851571i$	0.07	$1.20614 - 0.0630027i$	0.02	$1.70293 - 0.198065i$
0.12	$0.902565 - 0.0947457i$	0.08	$1.21651 - 0.0514301i$	0.025	$1.70506 - 0.214255i$
0.13	$1.03909 - 0.107478i$	0.09	$1.21431 - 0.0415960i$	0.03	$1.70405 - 0.232616i$
0.14	$1.01865 - 0.0859070i$	0.10	$1.20180 - 0.0347956i$	0.04	$1.69178 - 0.27573i$
0.15	$1.00159 - 0.0683552i$	0.11	$1.17941 - 0.0303883i$	0.05	$1.66379 - 0.327079i$
0.16	$0.983281 - 0.0666629i$	0.12	$1.14639 - 0.0274678i$	0.06	$1.61649 - 0.386106i$
0.17	$0.961166 - 0.0464981i$	0.13	$1.10110 - 0.0251206i$	0.07	$1.54442 - 0.451769i$
0.18	$0.933873 - 0.0396936i$	0.14	$1.04093 - 0.0224859i$	0.08	$1.43902 - 0.521872i$
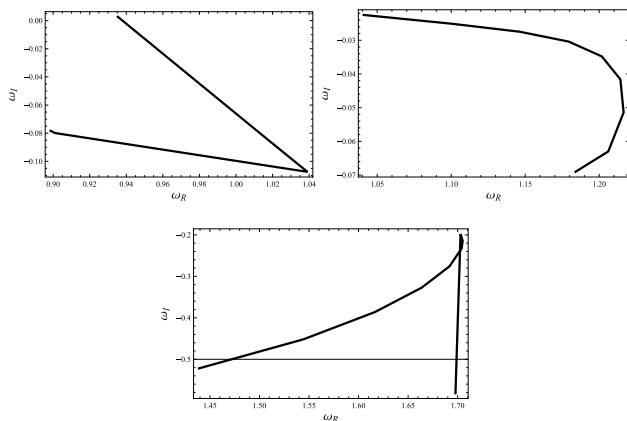
Fig. 3 QNM behavior for linearly charged BTZ black hole for dS space-time with $Q = 0.35$ for the massive parameter value $m = 0.9, 0.95, 1.0$. The sudden change in the slope can be treated as an indicative of a possible phase transition.

AdS space-time and compared. We have calculated the variation of QNMs with Λ for different values of the massive parameter m. For the dS space time, we have calculated the QNMs for the charges, $Q = 0.25$ and $Q = 0.35$. The black hole shows a phase transition in both of the cases, but the values of Λ at which the phase transition occurs are different for the two cases. For the AdS space-time also the variation of QNMs with Λ is looked into for the charge values, $Q = 0.1$ and $Q = 0.25$. It is found that for the case of $Q = 0.1$ no phase transition behavior is observed whereas, for $Q = 0.25$, the black hole shows a phase transition behavior. These results prompt one to check the variation of QNMs with Q for some fixed Λ for the dS and AdS space-time. It shows that a phase transition happens for a large range of charges for the dS space time whereas phase transition happens only for certain values of charge in the AdS space-time. In the next section we study the thermodynamic behavior of black holes and look for any phase transition of the system as the temperature, T of the system is varied.

3 Thermodynamics of the black hole

In this section, we study the thermodynamics of the linearly charged BTZ black hole in the (Anti) de Sitter space-time in massive gravity. The mass of the black hole, m_0, is given by the solution of the condition $f(r)|_{r \to r_H} = 0$, where r_H is the horizon radius, as

$$m_0 = m^2 c c_1 r_H + \Lambda r_H^2 - 2Q \ln\left(\frac{r_H}{\alpha}\right). \qquad (24)$$

The temperature of the black hole is given by $\frac{1}{4\pi} f'(r)|_{r \to r_H}$, which gives

$$T = \frac{cc_1 m^2}{4\pi} - \frac{Q}{2\pi r_H} + 4P r_H, \qquad (25)$$

where $P = \frac{\Lambda}{8\pi}$. Finally, the entropy is evaluated from the expression $S = \int_0^{r_H} \frac{1}{T} \frac{\partial m_0}{\partial r} dr$, which gives

$$S = 4\pi r_H. \qquad (26)$$

Then the equation of state, $P(V, T)$ can be obtained from the expression for the temperature, (25), as

$$P = \frac{Q}{8\pi r_H^2} + \frac{-cc_1 m^2 + 4\pi T}{16\pi r_H}. \qquad (27)$$

For an $(n + 2)$ dimensional massive gravity, the volume is given by [41], $V = (\frac{\partial H}{\partial P})_{S,Q} = \frac{V_n}{n+1} r^{n+1}$. With, $n = 1$, the calculation gives the horizon radius in terms of its volume as $r_H = (\frac{V}{8\pi})^{1/2}$.

To specify the phase transition it will be useful to introduce the Gibbs free energy as a Legendre transformation of enthalpy as

$$G = H - TS, \qquad (28)$$

where H is the enthalpy, T is the temperature given by (25) and S is the entropy given by (26). We use the black hole mass m_0 as the enthalpy since $H \equiv m_0$ rather than the internal energy of the gravitational system [22]. Substituting (24),

Table 3 QNMs of linearly charged BTZ black hole for different values of the massive parameter for AdS space-time with $Q = 0.1$

$m = 1.0$		$m = 1.05$		$m = 1.1$	
Λ	$\omega = \omega_R + \omega_I$	Λ	$\omega = \omega_R + \omega_I$	Λ	$\omega = \omega_R + \omega_I$
-0.06	$1.83077 - 5.78701i$	-0.05	$1.39873 - 7.68495i$		
-0.07	$1.70014 - 5.33444i$	-0.06	$1.29210 - 7.27705i$	-0.04	$0.75408 - 9.41718i$
-0.08	$1.53828 - 4.92198i$	-0.07	$1.14457 - 6.93423i$	-0.05	$0.63741 - 9.08170i$
-0.09	$1.34563 - 4.54476i$	-0.08	$0.95604 - 6.62556i$	-0.06	$0.48892 - 8.73203i$
-0.10	$1.11762 - 4.20206i$	-0.09	$0.72592 - 6.35819i$	-0.07	$0.21318 - 8.39613i$
-0.11	$0.84041 - 3.89983i$	-0.95	$0.58718 - 6.23146i$		
-0.12	$0.48197 - 3.66706i$	-0.10	$0.40624 - 6.12793i$		
-0.13	$0.81813 - 4.06506i$	-0.11	$1.57334 - 7.10865i$	-0.08	$2.18254 - 10.2207i$
-0.135	$0.75562 - 3.41486i$	-0.13	$1.12639 - 5.99601i$	-0.09	$1.44272 - 10.1043i$
-0.14	$0.32251 - 2.91165i$	-0.14	$0.86214 - 5.07753i$	-0.10	$1.41871 - 9.40952i$
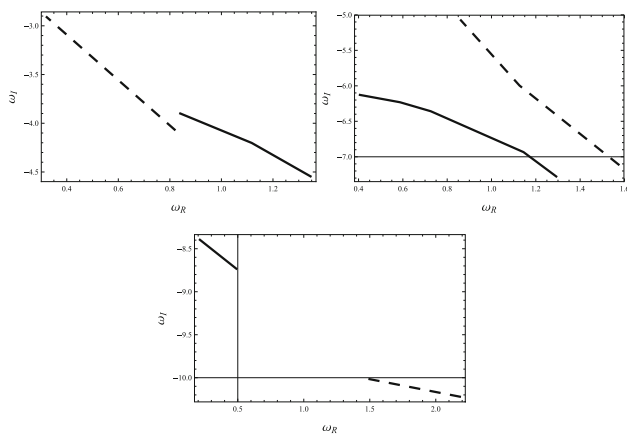
Fig. 4 QNM behavior for linearly charged BTZ black hole with charge $Q = 0.1$ for AdS space-time for the massive parameter value $m = 1, 1.05, 1.1$. The *bold lines* represent the behavior of QNMs before the inflection point and the *dotted lines* represent the behavior of QNMs after the inflection point. The behavior of QNMs is seen to be similar in the plots. There is not much difference in the slope of the curves

(25), and (26) in (28), we get an expression for the Gibbs free energy:

$$G(T, \Lambda) = 2Q + \Lambda r_H^2 - 2Q \ln \left(\frac{r_H}{\alpha} \right). \tag{29}$$
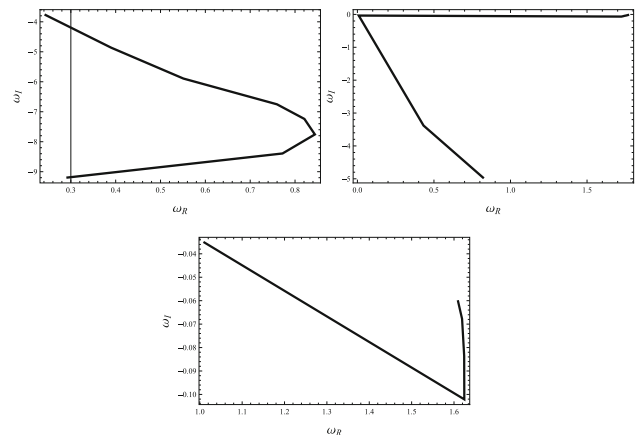

Fig. 5 QNM behavior for linearly charged BTZ black hole for $Q = 0.25$ the massive parameter value $m = 0.95, 1.0, 1.05$.

Figure 8 shows the variation of Gibbs free energy with temperature plotted using (25) and (29). The top of the figure shows the G–T plot for $P = \frac{\Lambda}{8\pi} = 0.001$ (de Sitter case). It can be seen that for negative T the Gibbs free energy has a maximum value and, as T increases, the value of G decreases, reaches zero at some particular value of T, and then takes neg-

Table 4 QNMs of linearly charged BTZ black hole for different values of the massive parameter for AdS space-time with $Q = 0.25$

$m = 0.95$		$m = 1.0$		$m = 1.05$	
Λ	$\omega = \omega_R + \omega_I$	Λ	$\omega = \omega_R + \omega_I$	Λ	$\omega = \omega_R + \omega_I$
0.01	$0.292587 - 9.19482i$	0.13	$0.820054 - 4.96149i$	0.29	$1.01098 - 0.0351877i$
0.02	$0.772162 - 8.39220i$	0.15	$0.431983 - 3.38060i$	0.31	$1.02868 - 0.0148701i$
0.03	$0.844245 - 7.75702i$	0.17	$0.00879691 - 0.0348464i$	0.32	$1.04119 - 0.00215093i$
0.04	$0.820904 - 7.24016i$	0.19	$1.72429 - 0.0660172i$	0.33	$1.62431 - 0.102106i$
0.05	$0.759655 - 6.75177i$	0.20	$1.73419 - 0.0561830i$	0.34	$1.62400 - 0.083530i$
0.07	$0.551068 - 5.89321i$	0.21	$1.74461 - 0.043151i$	0.35	$1.61905 - 0.067770i$
0.09	$0.390010 - 4.86350i$	0.22	$1.75581 - 0.0330092i$	0.36	$1.60957 - 0.060276i$
0.11	$0.243717 - 3.77402i$	0.23	$1.76769 - 0.0186321i$		

Table 5 Table showing the variation of QNMs with Q in the dS space-time

Q	ω
0.15	$4.47348 - 0.19884i$
0.20	$4.33915 - 0.108836i$
0.25	$0.0930679 - 0.0668980i$
0.30	$1.54638 - 0.132502i$
0.35	$1.68971 - 0.172263i$
0.40	$0.0325096 - 0.466834i$

Fig. 7 Variation of QNMs with charge Q for AdS space time

Fig. 6 Variation of QNMs with charge Q for the dS space time

Table 6 Table showing the variation of QNMs with Q in the AdS space

Q	ω
0.05	$1.12930 - 9.66585i$
0.10	$1.14048 - 9.54589i$
0.15	$2.42998 - 12.8629i$
0.20	$3.49176 - 14.0316i$
0.25	$3.64711 - 13.9835i$
0.30	$0.294699 - 9.56518i$
0.35	$0.557735 - 9.42807i$
0.40	$0.792729 - 9.21181i$
0.45	$0.940783 - 9.04476i$
0.50	$1.03930 - 8.88485i$
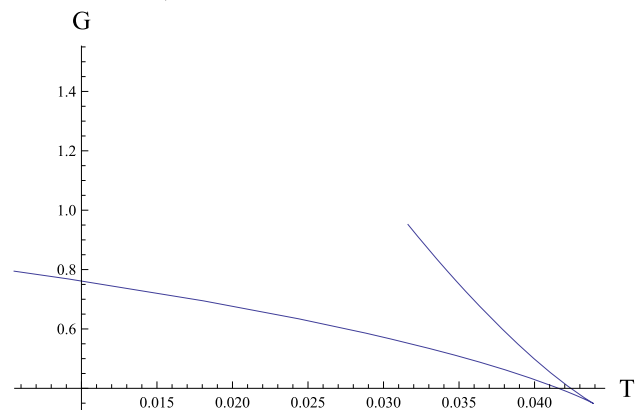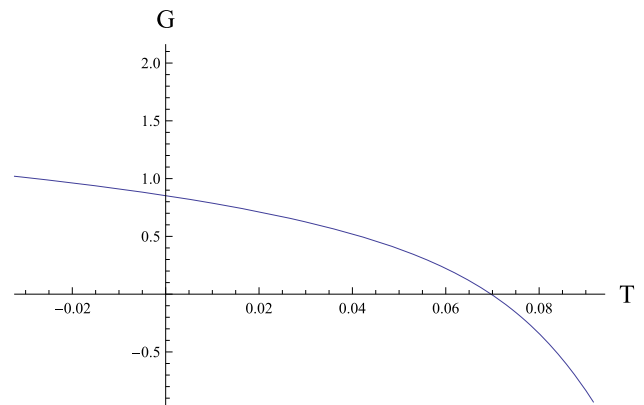
Fig. 8 Variation of Gibbs free energy with temperature for the dS space-time (*top*) and AdS space tome (*bottom*)

ative values. Thus G varies from positive to negative values which indicates a possible phase transition. The bottom plot shows variation of G with T for $P = -0.001$ (Anti de Sitter case). The plot lies in the positive Gibbs free energy region and shows a cusp like behavior.

Figure 9 shows the variation of pressure, P and temperature, T with the horizon radius, r_{H}, for fixed values of temperature and pressure, respectively. The top of Fig. 9 shows the variation of temperature with r_h given by (25) for the pressure values $P = -0.003, -0.002, -0.001, 0.001$, and

0.002. The bottom of Fig. 9 shows the variation of pressure with r_h given by (27) for the fixed values of temperature of $T = -0.3, -0.2, -0.1, 0.1$, and 0.2.

More details regarding the phase transition can be extracted from the entropy of the system. The temperature–entropy relation would be worth looking at. For that the expression for r_{H} derived from (26) is substituted into (25) so that we get an expression relating the entropy and temperature,
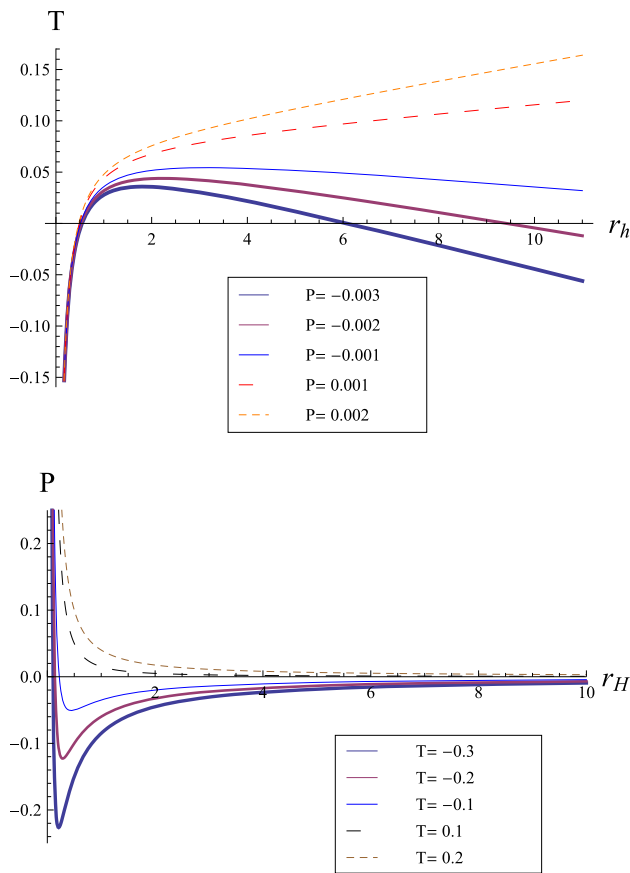
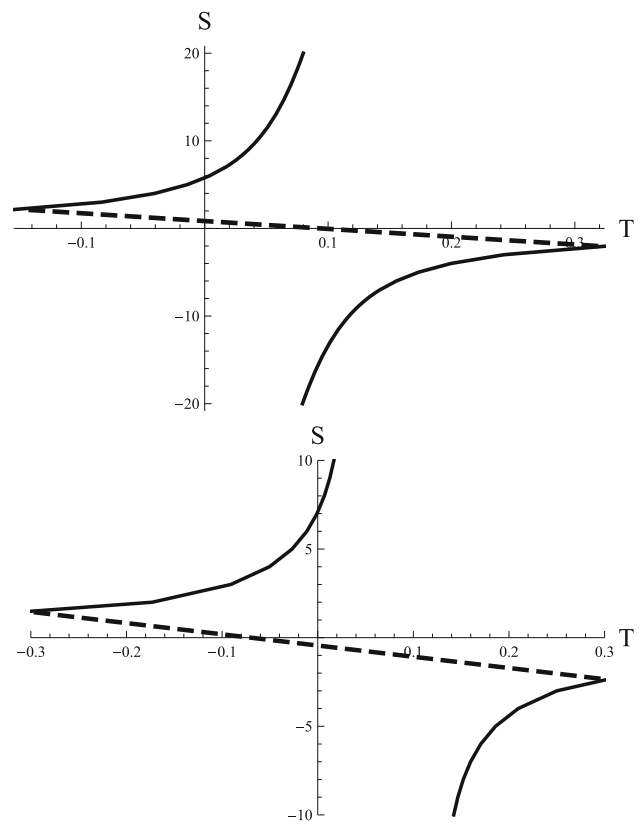**Fig. 9** *Top* Variation of T with r_H. *Bottom* Variation of P with r_H

Fig. 10 The variation of thermal entropy with temperature for the $\Lambda = 0.1$ (*top* which is dS space-time) and -0.1 (*bottom* which is AdS space-time)

$$T = -\frac{2Q}{S} + \frac{2\pi cc_1 m^2 + \Lambda S}{8\pi^2}. \tag{30}$$

Figure 10 shows the S–T plots for the values $\Lambda = 0.1$ and $\Lambda = -0.1$, with the parameter values $m_0 = c = c_1 = 1$, $\alpha = 1$, $Q = 0.25$, and $m = 1$. It can be seen that there is a discontinuity at some particular value of T in both cases and hence both of them can be said to show phase transition behavior.

Now, in order to study the stability of the phases or the feasibility of the above phase transitions, it may be worth looking at the behavior of the specific heat with temperature. If the behavior of the heat capacity indicates that as the temperature varies the heat capacity makes a transition from negative values to positive values, the system undergoes a phase transition. A negative heat capacity represents an unstable state, while a positive value of the specific heat implies a stable state. The specific heat is given by

$$C_Q = \frac{T}{\left(\frac{\partial T}{\partial S}\right)_Q}, \tag{31}$$

which from (26) and (30) leads to

$$C_Q = 2\pi r_H \frac{\left(-2Q + r_H\left(m^2 + 2r_H\Lambda\right)\right)}{Q + r_H^2\Lambda}. \tag{32}$$

The plots of the specific heat versus temperature for $\Lambda = 0.1$ (de Sitter) and $\Lambda = -0.1$ (Anti de Sitter) are given in Fig. 11 for the parameter values $m = c = c_1 = 1$ and $Q = 0.25$. From the plot it can be clearly understood that for $\Lambda = 0.1$ the specific heat changes from negative to positive values, indicating a phase transition from unstable to stable configuration. For $\Lambda = -0.1$, we can say that it somewhat shows a phase transition behavior. However, it is observed that for given constant parameter values the black holes in AdS space-time show this phase transition behavior only for a very small range of Λ values whereas in dS space-time it shows a phase transition for a wide range of Λ values.

It would also be worth noting the variation of the behavior of specific heat with Q. For this purpose, we have plotted the variation of the specific heat with temperature for $Q = 0.1, 0.25, 0.5, 0.6$ for dS space-time; the other parameters remain the same. See Fig. 12.

It can be seen that up to $Q = 0.5$ it shows a phase transition and then after reaching $Q = 0.6$, it no more shows any phase transition. Also it is found that above this value no phase transition is observed.

The variation of the behavior of the specific heat with Q for the AdS space-time for the values $Q = 0.1, 0.25, 0.3, 0.4$ is shown in Fig. 13.
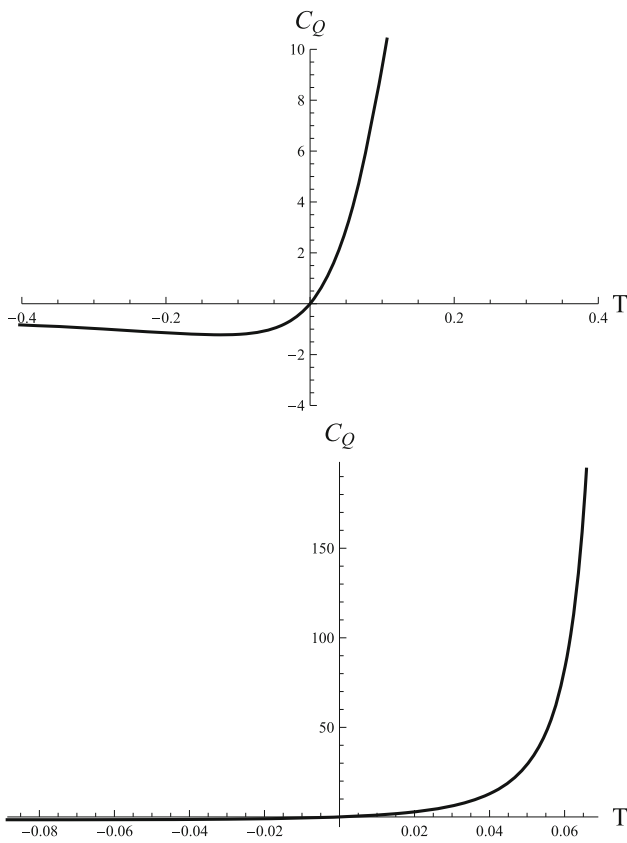
Fig. 11 Figure showing the variation of the specific heat with temperature for $\Lambda = 0.1$ (*top*) and $\Lambda = -0.1$ (*bottom*)
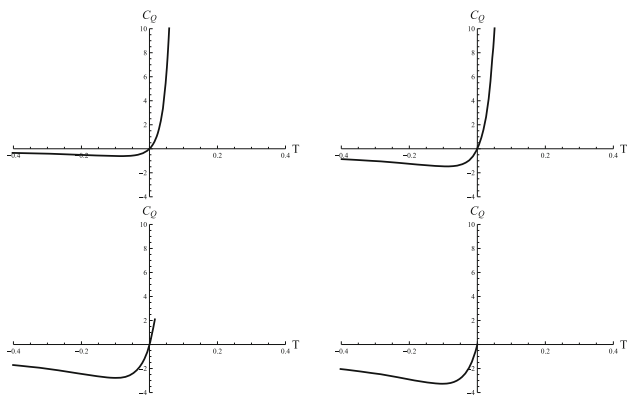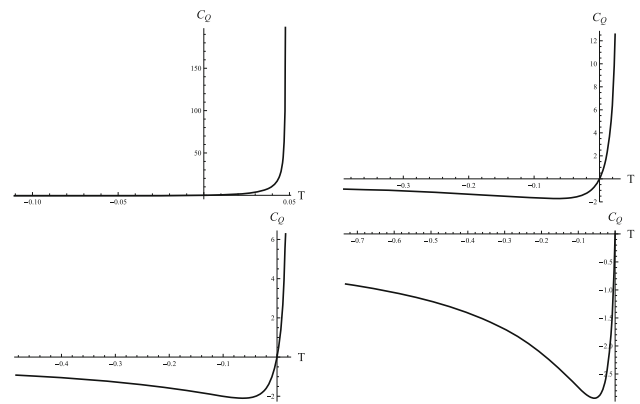

Fig. 12 The variation of the specific heat with temperature for $Q = 0.1, 0.25, 0.5, 0.6$, respectively, from top left in dS space-time

It can be seen that for $Q = 0.1$ it does not show any phase transition and for $Q = 0.25$ and $Q = 0.3$ it shows a phase transition and then after reaching $Q = 0.4$, it no more shows any phase transition. Also it is found that above this value no phase transition is observed. From this it can also be concluded that AdS space-time shows a phase transition only for a small range of Q when compared with the dS space-time.

Fig. 13 The variation of the specific heat with temperature for $Q = 0.1, 0.25, 0.3, 0.4$, respectively, from top left in AdS space time

Thus from the specific heat plots phase transition is observed in the de Sitter space-time for the values of charge $Q = 0.1$ to $Q = 0.5$ and no phase transition is observed above the value $Q = 0.6$. In the AdS case, the phase transition is not observed for $Q = 0.1$ and values above $Q = 0.4$ and shows a phase transition for $Q = 0.25$ and $Q = 0.3$. These results are in accordance with Sect. 2.

4 Conclusion

In this paper we have calculated the QNMs for a linearly charged BTZ black hole in massive gravity. The values of the parameters are so chosen that in the metric function the massive parameter dominates. It is found that in the de Sitter space-time, as the cosmological constant Λ is increased, the quasi-normal frequencies vary continuously and then after reaching a particular value of $\Lambda(= 0.1)$, their behavior is found to be abruptly changing afterwards. This is shown in the $\omega_{\mathrm{I}}-\omega_{\mathrm{R}}$ plot where there is a drastic change in the slope of the curve after a particular value of Λ. This can be seen as a strong indication of a possible phase transition occurring in the system. When the massive parameter m is increased, a similar behavior is found but the Λ at which the change of behavior of QNMs is found is shifted to a higher value ($\Lambda = 0.28$). Also, it can be inferred that the variation of the massive parameter will only alter the point at which the phase transition happens. For different values of Q the phase transition occurs for different values of Λ.

The QNMs for an (Anti) de Sitter space-time are also calculated and the behavior of their quasi-normal frequencies is analyzed. For $Q = 0.1$ the behavior of QNMs showed an inflection point but no phase transition. However, for $Q = 0.25$ it showed a phase transition. Thus it is seen that the phase transition behavior is found to be dependent on Q for the AdS case. It is also observed by studying the variation of QNMs with Q that AdS space-time shows a phase transition only for certain limited ranges of Q compared to the dS case.

The thermodynamics of such black holes in the dS space is then looked into. The behavior of the specific heat showed a phase transition for the dS case for a wide range of Q whereas for the AdS space-time phase transition is shown only for a limited range of Q.

References

1. S. Capozziello, M. De Laurentis, Phys. Rep. **509**, 167 (2011). arXiv:1108.6266
2. T. Clinton, Phys. Rep. **513**, 1 (2012)
3. D. Mattingly, Liv. Rev. Rel. **8**, lrr-2005-5 (2005)
4. M. Fierz, W. Pauli, Proc. R. Soc. Lond. Ser. A **173**, 211232 (1939)
5. H. van Dam, M.J.G. Veltman, Nucl. Phys. B **22**, 397 (1970)
6. V.I. Zakharov, JETP Lett. **12**, 312 (1970)
7. A.I. Vainshtein, Phys. Lett. B. **39**, 393 (1972)
8. D.G. Boulware, S. Deser, Phys. Rev. D **6**, 3368 (1972)
9. C. de Rham, G. Gabadadze, A.J. Tolley, Phys. Rev. Lett. **106**, 231101 (2011)
10. M.S. Volkov, Class. Quantum Grav. **30**, 184009 (2013)
11. H. Kodama, I. Arraut, Prog. Theor. Exp. Phys., 023E0 (2014). arXiv:1312.0370
12. S.G. Ghosh, L. Tannukij, P. Wongjun, Eur. Phys. J. C. **76**, 119 (2016)
13. P. Prasia, V.C. Kuriakose, Gen. Relat. Gravit. **48**, 89 (2016)
14. D. Vegh, CERN-PH-TH/2013-357 (2013). arXiv:1301.0537
15. S.W. Hawking, D.N. Page, Commun. Math. Phys. **87**, 577 (1983)
16. P.C.W. Davies, Rep. Prog. Phys. **41**, 1313 (1978)
17. D.J. Gross, M.J. Perry, L.G. Yaffe, Phys. Rev. D **25**, 330 (1982)
18. S. Carlip, Int. J. Mod. Phys. D **23**, 1430023 (2014)
19. P. Brian, Dolan. Class. Quantum Grav. **28**, 125020 (2011)
20. K. Ghaderi, B. Malakolkalami, Nucl. Phys. B **903**, 10 (2016)
21. J. Suresh, R. Tharanath, N. Varghese, V.C. Kuriakose, Eur. Phys. J. C. **74**, 2819 (2014)
22. F. Capelaa, P.G. Tinyakov, JHEP **1104**, 042 (2011). arXiv:1102.0479
23. R.G. Cai, Y.P. Hu, Q.Y. Pan, Y.L. Zhang, Phys. Rev. D. **91**, 024032 (2015)
24. M. Banados, C. Teitelboim, J. Zanelli, Phys. Rev. Lett. **69**, 1849 (1992)
25. M. Banados, M. Henneaux, C. Teitelboim, J. Zanelli, Phys. Rev. D **48**, 1506 (1992)
26. N. Cruz, S. Lepe, Phys. Lett. B **593**, 235 (2004)
27. M. Cadoni, M. Melis, Found. Phys. **40**, 638 (2010). arXiv:0907.1559
28. A. Chamblin, R. Emparan, C. Johnson, R. Myers, Phys. Rev. D **60**, 064018 (1999)
29. M. Cadoni, M. Melis, M.R. Setare, Class. Quantum Grav. **25**, 195022 (2008)
30. M.R. Setare, H. Adami, Phys. Rev. D **91**, 104039 (2015)
31. C.V. Vishveswara, Nature **227**, 936 (1970)
32. S. Chandrasekhar, S. Detweiler, Proc. R. Soc. Lond. **A344**, 441 (1975)
33. V. Cardoso, J.P.S. Lemos, Phys. Rev. D **63**, 124015 (2001)
34. D. Maity et al., Nucl. Phys. B **839**, 526 (2010). arXiv:0909.4051v2
35. S.H. Hendi, B. Eslam Panah, S. Panahiyan, JHEP **05**, 029 (2016). arXiv:1604.00370v1
36. I.G. Moss, J.P. Norman, Class. Quantum Grav. **19**, 2323 (2002)
37. H. Ciftci, R.L. Hall, N. Saad, Phys. Lett. A **340**, 388 (2005)
38. H.T. Cho, A.S. Cornell, D. Jason, T.R. Huang, N. Wade, Adv. Math. Phys. **2012**, 281705 (2012)
39. H.T. Cho, A.S. Cornell, D. Jason, N. Wade, Class. Quantum Grav. **27**, 155004 (2010)
40. W. Naylor, Black holes: AIM. http://wade-naylor.com/aim/
41. J. Xi, L. Cao, Y.P. Hu, Phys. Rev. D **91**, 124033 (2015)